

21-cm Intensity Mapping with FAST

George F. Smoot,^{a,b} Ivan Debono^{c,d}

^cParis Centre for Cosmological Physics, APC (CNRS), Université Paris Diderot, Université Sorbonne Paris Cité, 75013 France

^bPhysics Department and Lawrence Berkeley National Laboratory, University of California, Berkeley, CA 94720, USA

^cAPC, AstroParticule et Cosmologie, Université Paris Diderot, CNRS/IN2P3, CEA/Irfu, Observatoire de Paris, Sorbonne Paris Cité, 10 rue Alice Domon et Léonie Duquet, 75205 Paris Cedex 13, France.

^dLESIA, Observatoire de Paris, CNRS, UPMC, Université Paris Diderot, 5 place Jules Janssen, 92195 Meudon, France.

E-mail: gfsmoot@lbl.gov, ivan.debono@apc.univ-paris7.fr

Abstract. This paper describes a program to map large-scale cosmic structures on the largest possible scales by using FAST[1] to make a 21-cm (red-shifted) Intensity Map of the sky for the range $0.5 < z < 2.5$. The goal is to map to the angular and spectral resolution of FAST a large swath of the sky by simple drift scans with a transverse set of beams. This approach would be competitive to galaxy surveys and could be completed before SKA could begin a more detailed and precise effort. The science would be to measure the large-scale structure on the size of the baryon acoustic oscillations and larger scale and the results would be competitive to its contemporary observations and significant. The survey would be uniquely sensitive to the potential very large-scale features from GUT-scale Inflation and complementary to the CMB observations.

Contents

1	Introduction	1
1.1	Goals and Outline	2
2	Concept and Techniques	3
2.1	Required System Sensitivity	3
2.2	Drift and 1/f noise	4
2.3	Expected Signal Level	5
2.4	Mapping Angular Resolution to Spatial Resolution	6
2.4.1	FAST Angular Resolution	6
2.4.2	Angular Resolution and Physical Size	6
2.5	Foregrounds - Galactic and Extragalactic	7
2.6	Removal of Foregrounds	10
3	Survey Parameters	11
3.1	Survey 1: Proof of Concept 2-D Map	11
3.2	Survey 2: Large Scale 3-D Perturbation Mapping	13
4	Anticipated Science	14
4.1	Anticipated Science: Motivated models of large-scale perturbations	16
4.2	Anticipated Science: Observing BAO features	21
4.3	Anticipated Science: Testing General Relativity	21
4.4	Anticipated Ancillary Science:	21
4.4.1	Radio Transients:	21
4.4.2	Pulsars:	21
4.4.3	Galactic Magnetic Fields:	22
5	Conclusions and Future	22

1 Introduction

This paper describes a possible program to map large-scale structures on the largest possible scales using FAST[1] to make a 21-cm (red-shifted) Intensity Map of the sky. It has long been recognized that mapping the 21-cm hydrogen intensity is a very good way to measure the very large scale perturbation power spectrum[2] and that on scales above 8 to 10 Mpc, the hydrogen gas represents a fair and unbiased sample of the large-scale matter distribution[3].

Using the 21-cm line of hydrogen, observed all-sky and across the redshift range from 0 to 5, the large-scale structure of the Universe can be mapped in three dimensions. (At the higher redshifts the Lyman-alpha line of hydrogen is likely to be a better mapping tool, though it is good to have strong overlap and the more full map that the 21-cm intensity maps can provide.) This can be accomplished by studying specific

intensity with resolution ~ 5 Mpc, rather than via the usual galaxy redshift surveys. Intensity mapping measures the collective emission of many galaxies without detecting and studying individual galaxies.

FAST data will be quite complementary to galaxy redshift and weak lensing surveys. The FAST data do well at covering the large scales (> 10 Mpc, $k < 0.003h\text{Mpc}^{-1}$), while the galaxy and weak lensing surveys are more precise at small scales (< 100 Mpc, $k > 0.01h\text{Mpc}^{-1}$).

The data set can be analyzed to determine Baryon Acoustic Oscillation features and power spectra, in order to address the following questions: What is the nature of Dark Energy? How does Gravity effect very large objects? Is there a departure from General Relativity? What is the composition our Universe? Does the Dark Matter behave as expected? The same data set can be used to search for and catalog time variable and transient radio sources. But most importantly, studying the hydrogen emission is probably our only real tool, besides the CMB, to study the very large scale perturbations and detect anticipated features that might appear there for transitions in the very early Universe.

The large-scale structure of the Universe supplies crucial information about physical processes at early times. Unresolved maps of the intensity of 21-cm emission from neutral hydrogen HI at redshifts $z \sim 1 - 5$ are the best hope of accessing new ultra large-scale information, directly related to the early Universe. It is possible to look for very large scale features induced by such processes as the GUT symmetry-breaking. An appropriate HI intensity experiment may detect the large-scale effects of primordial non-Gaussianity, placing stringent bounds on different models of inflation. It may be possible to place tight constraints on the non-Gaussianity parameter f_{NL} , with an error close to $\sigma_{f_{NL}} \sim 1$ [4].

1.1 Goals and Outline

The goal is to make an intensity map of 21-cm hydrogen emission over a significant redshift range (z from about 0.5 to 2.5, which corresponds to frequency coverage of about 400 MHz to 1 GHz) with sufficient angular and frequency resolution both to observe the baryon acoustic oscillations (BAO) and to observe any features in the very large scales primordial perturbation spectrum. Such a survey is very complementary to galaxy surveys and provides information on the very early Universe that is difficult to obtain any other way.

We show here that mapping to the angular and spectral resolution of FAST a large swath of the sky by simple drift scans with a transverse set of beams can be sufficient to meet these goals. This paper outlines the major features necessary: receivers with bandwidths stretching from 1.42 GHz (1 GHz would likely be sufficient to get most of the science as the volume at lower redshifts is not so great) down as low as is reasonable, but certainly to about 0.4 GHz. In the longer term one may well work to extend the bandwidth to even lower frequencies and thus to higher redshift.

It would be best to have the system temperature 20K or less so as to map most quickly and make best use of the valuable telescope time. The system temperature will necessarily be a bit higher at lower frequencies because of the galactic foreground signal.

A single 40-degree swatch by drift scan takes a minimum of 48 days of observations with a linear array of 10 receivers. However, if things work well, then one would want to extend to about two years of observations. This approach would be competitive with galaxy surveys, and CHIME[8], and could be completed before SKA could begin a more detailed effort. The science would be to measure the large-scale structure on the size of the baryon acoustic oscillations and larger scale. The survey would be uniquely sensitive to the potential very large-scale features from GUT-scale Inflation and complementary to the CMB observations.

2 Concept and Techniques

The concept is to map the sky in rest-frame 21-cm wavelength (1.42 GHz and lower) with an angular resolution of about 5 arcmin and δz of approximately 0.001 or 0.1% in frequency. This can be translated into a real-space map and power spectrum of the primordial perturbations, which we believe are from Inflation, e.g.[5]. These perturbations are processed through the baryon acoustic oscillations and the damping of structure formation. We believe that we understand these processes, but the data can be used first to check the baryon acoustic oscillations, using them as a standard ruler and testing the Dark Energy acceleration of the Universe and potential modifications to General Relativity. If these are in agreement, the primordial power perturbations can easily be unfolded and tested against the predictions of Inflation and GUT perturbed inflationary models as the features should show up both in real space and in the power spectrum.

2.1 Required System Sensitivity

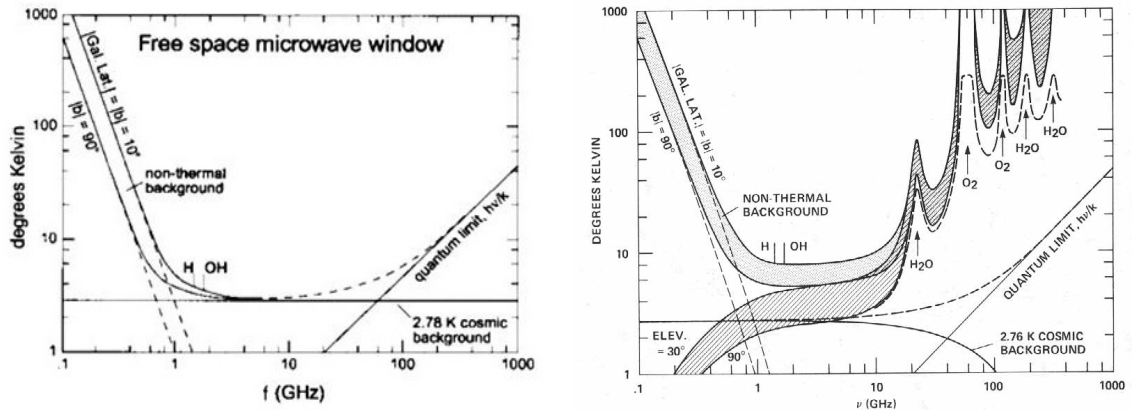


Figure 1. Plot showing representative signal expected from the CMB and for the galaxy at two galactic latitudes, as a function of frequency. On the right the plot includes estimated atmospheric emission. Figures from reference[6].

Figure 1 shows the relative brightness from the major background of synchrotron radiation. It is estimated to be about 0.3 to 1 K at 1.4 GHz near the galactic plane

to substantially less well off the plane. At 0.41 GHz it is about 3-10 K. This means that the total background temperature including CMB is about 4 to 15 K and that the receivers should not contribute significantly to this total or it would slow the mapping speed of the telescope. One would wish for a complete system with an effective noise temperature of about 20 K.

The basic noise-scale would be given by

$$\delta T_{\text{rms}} = \frac{T_{\text{sys}}}{\sqrt{Bt}} \simeq \frac{20\text{K}}{(0.003 \times 10^9 \times 4)^{1/2}} = 3.4 \text{ mK} \quad (2.1)$$

assuming an integration time of 4 seconds and a total system temperature of 20 K and a pixel bandwidth in the z direction of 0.3% . In 4 seconds the earth's rotation sweeps through about 1 arcmin.

Pixel Size, Volume, and sensitivity: Let us consider a pixel size of $5 h^{-1}$ Mpc as our standard sized comoving sample. (This gives a Nyquist-size sample for $10 h^{-1}$ Mpc wavelength and above.) In 20 seconds the rotation of the earth sweeps through our canonical 5 arcmin which typically in the redshift range of 1 to 2 gives the $5 h^{-1}$ Mpc size. Thus a single drift scan integration time is about 20 seconds. In the redshift direction a $5 h^{-1}$ Mpc in depth pixel is $\delta z = 5 h^{-1} \text{Mpc} \times H/c \sim 10^{-3} = 0.1\%$. Putting this together we have for each receiver channel

$$\delta T_{\text{rms pixel}} = 20\text{K}/(20 \times 10^{-3} \times 1.42 \times 10^9/(1+z))^{1/2} = 3.75\sqrt{(1+z)} \text{ mK}. \quad (2.2)$$

The BAO scale is around 100 Mpc so that one gets a reasonable number of samples (about 400, greater including z direction) in each BAO feature and thus an expected noise of around 0.2 mK for a BAO feature. Even with the array of 20 receivers, one still is lacking by a factor of two in what one would desire for sensitivity. To gain that would require a minimum of four days per elevation scan.

2.2 Drift and 1/f noise

The discussion thus far has only considered receiver white noise. In practice, for long periods there are drifts in the receiver performance particularly in gain that must be considered. This is generally known as 1/f noise since that is the dependence that does not integrate down and can leave long-wave signals in the observations. The standard technique is to make a differential observation or a correlation receiver which again means differencing two portions of the sky or an equivalent temperature reference load. Ideally one would use something like the north celestial pole region as the reference point either in a difference (e.g. Dicke radiometer) or correlation receiver. In the Dicke radiometer case one suffers a factor of two in sensitivity. With the correlation receiver one can break even or suffer $\sqrt{2}$ in sensitivity.

One could consider a wide beam pointing directly upward to compare with the high resolution beam via the downward-pointing feed. This would give an average over the HI 21-cm emission that will be pretty much the same over all the sky and average out most of the extragalactic point sources. It also looks through the same column of atmosphere allowing cancelation of that signal. However, the Galactic synchrotron

emission varies on the very large scale on the sky so that there would be primarily a large quadrupolar feature in the observations plus extra signal on the galactic plane. This can probably be handled to first order by a smooth parametrization modelling.

One can consider frequency switching and/or using symmetric matching beams as references but this requires a somewhat more complicated scanning and data processing system but might well be worth the effort if the differential system over-complicates the receiver cabin.

The opposite direction differential correlation receiver system is probably the best option but a switching differential will work well too. For the purposes of this paper we assume that a simple solution exists in this form or in a synthesis form and use the numbers to provide a scale and reference for a more detailed design. Luckily, there have been significant advances in room-temperature low-cost receivers with adequate noise figure, which today cost as little as 60 yuan each, and advances in FPGA that make processing the signal into 0.1% frequency bands (roughly 1 MHz) readily achievable so that one can easily envisage adding 20 or so receivers covering this frequency range to the existing system. The major cost is the effort to assemble and install the receivers and antennas.

2.3 Expected Signal Level

There have been a number of estimates of the expected 21-cm intensity mapping signal level. A recent paper [18] gives $T_b = \bar{T}_b(1 + \delta_{\text{HI}})$ which is given by

$$\bar{T}_b = \frac{3}{32\pi} \frac{hc^3 A_{10}}{k_B m_p^2 \nu_{21}} \frac{(1+z)^2}{H(z)} \Omega_{\text{HI}}(z) \rho_{c,0}. \quad (2.3)$$

and the fluctuations are given by

$$\delta T^S(\theta_p, \nu_p) = \bar{T}_b(z) \delta_{\text{HI}}(\mathbf{r}_p, z).$$

The rough estimate of the biased neutral hydrogen density is then

$$\Omega_{\text{HI}} b_{\text{HI}} = 4.3 \pm 1.1 \times 10^{-4} \quad \delta_{\text{HI}} = b_{\text{HI}} \star \delta_M$$

Assuming that the peculiar velocity gradient and v/c terms are small for these large pixels, we finally get

$$T_b(\nu, \Delta\Omega, \Delta\nu) \approx \bar{T}_b(z) \left[1 + b_{\text{HI}} \delta_m(z) - \frac{1}{H(z)} \frac{dv}{ds} \right]$$

$$\bar{T}_b(z) \approx 566h \left(\frac{H_0}{H(z)} \right) \left(\frac{\Omega_{\text{HI}}(z)}{0.003} \right) (1+z)^2 \mu\text{K}.$$

That is to say, the typical scale of the HI 21-cm signal is around 0.5 mK.

A more specific case of data analysis where one averages over a radial bin and measures the power spectrum in redshift is considered in [19]. The projected error on a power spectrum measurement average over a radial bin in k -space of width Δk is

$$\frac{\sigma_P}{P} = \sqrt{2 \frac{(2\pi)^3}{V_{\text{sur}}} \frac{1}{4\pi k^2 \Delta k} \left(1 + \frac{\sigma_{\text{pix}}^2 V_{\text{pix}}}{[\bar{T}(z)]^2 W(k)^2 P} \right)}, \quad (2.4)$$

where V_{sur} is the survey volume, σ_{pix} is the pixel noise over a nominal bandwidth of $\Delta f = 1\text{MHz}$ and $W(k)$ is the angular window function. The survey volume is a function of the observed patch of the sky Ω_{sur} and is given by

$$V_{\text{sur}} = \Omega_{\text{sur}} \int_{z_{\text{min}}}^{z_{\text{max}}} dz \frac{dV}{dz d\Omega}, \quad (2.5)$$

where

$$\frac{dV}{dz d\Omega} = \frac{cr(z)^2}{H_0 E(z)}. \quad (2.6)$$

$\bar{T}(z)$ is the average temperature:

$$\bar{T}(z) = 44 \mu\text{K} \left(\frac{\Omega_{\text{HI}}(z)h}{2.45 \times 10^{-4}} \right) \frac{(1+z)^2}{E(z)} = 440 \mu\text{K} \left(\frac{H_0}{H(z)} \right) \left(\frac{\Omega_{\text{HI}}(z)h}{2.45 \times 10^{-3}} \right) (1+z)^2. \quad (2.7)$$

Ω_{HI} is the HI density relative to the present day critical density and $E(z) = H(z)/H_0$.

The first portion is simply the sample variance of the number of modes included in the survey. The second term takes into account the signal-to-noise ratio on a pixel. That is to say, if the noise variance on a pixel is larger than the signal in the pixel, the net error on the power spectrum is increased by that factor. That is why getting the receiver noise down to minimum addition to the background is so relevant.

2.4 Mapping Angular Resolution to Spatial Resolution

2.4.1 FAST Angular Resolution

For a full dish illumination the resolution at 21-cm wavelength is about $\theta = 1.22\lambda/d = 1.22 \times 0.21/500 = 5.21 \times 10^{-4}\text{radians} = 1.76 \text{ arcmin}$. The angular resolution scales with redshift as $\theta(z) = 1.2\lambda(z)/d = 1.76(1+z) \text{ arcmin}$. Thus the angular resolution rises from 1.76 arcmin to just over 5 arcmin at a redshift of 2 corresponding to a wavelength of $\lambda(z) = (1+z) 21\text{-cm}$ or, $\lambda_{z=2} = 63 \text{ cm}$ corresponding to a frequency of $f = 1.42\text{GHz}/(1+z)$, or $f_{z=2} = 473 \text{ MHz}$. For $z = 2.5$, these are $f_{z=2.5} = 405.7 \text{ MHz}$ and $\lambda_{z=2.5} = 73.5 \text{ cm}$, and for $z = 0.5$, $f_{z=0.5} = 946.7 \text{ MHz}$ and $\lambda_{z=0.5} = 31.5 \text{ cm}$. Now it is possible to use the full 500-m aperture for the vertical drift scans but to extend the width of the survey, it is either necessary to go to a smaller illumination as one moves off center and probably to build the proposed ground screen especially on the north side of the telescope to look further south.

2.4.2 Angular Resolution and Physical Size

At a redshift of about $z=1.5$ the size 8 Mpc is about 18 arcmin in angle or a bit larger. Thus at $z=2$ we have 5 arcmin resolution. This gives us a bit better than Nyquist sampling, which is good for making maps and power spectra.

Figure 14 shows the angular size versus redshift for a fixed physical size. For our universe, the angular size is relatively constant for redshift 1 to 2 for the mapping survey. For instance, a galaxy cluster with a size of about 1 Mpc will never subtend an angle less than about $4 h$ arcmin regardless of its distance from the observer. Thus

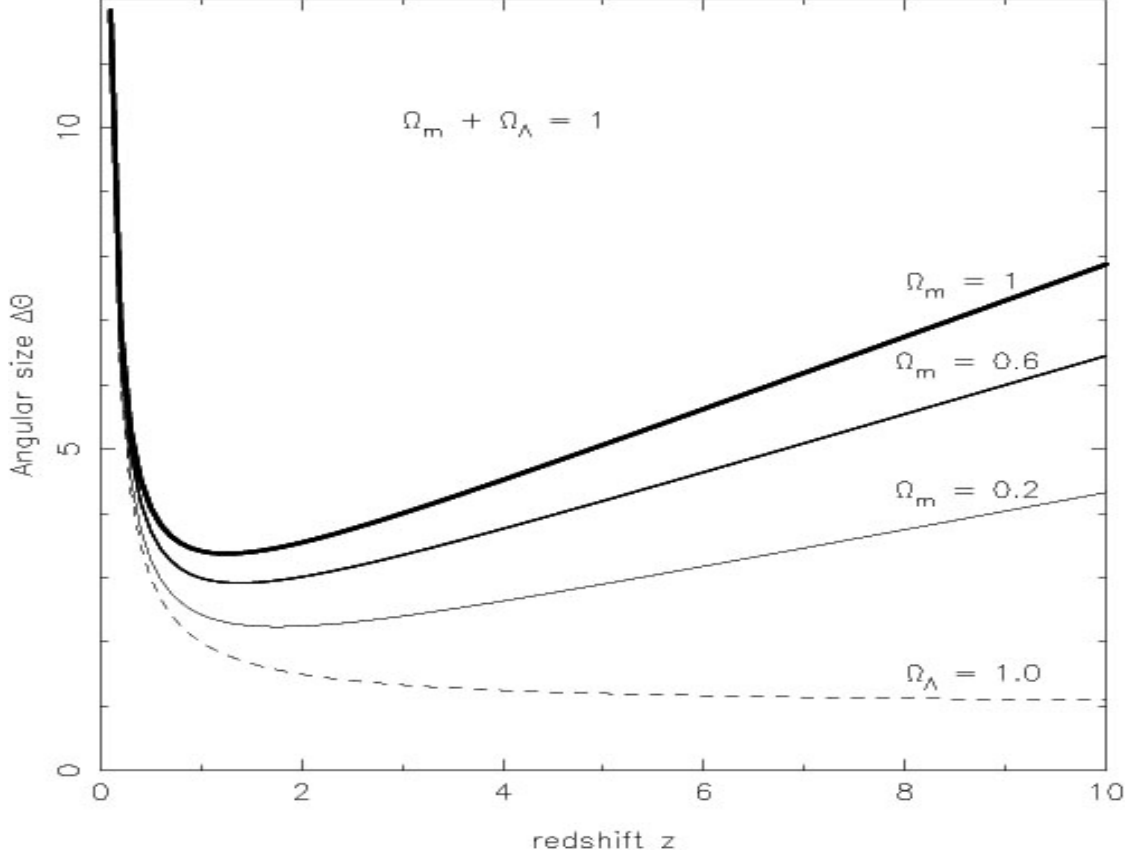


Figure 2. The angular size is shown as a function of cosmological redshift z for flat cosmological models with a cosmological constant $\Omega_m + \Omega_\Lambda = 1$. Heavier lines correspond to larger values of Ω_m . For comparison we also show (dashed line) the angular size in a de Sitter universe ($\Omega_\Lambda = 1$). The current best fitted models of our Universe give $\Omega_m \sim 0.3$ and thus we expect that the angular size of objects in the range from $1 < z < 3$ are relatively unchanging. Figure from reference[7].

FAST could also be used to search for galaxy clusters in a way that is competitive with the SZ searches but mapping the intensity is a more direct and straightforward way to look at the large-scale structure.

The BAO scales corresponds to an angles of about 2° at $z = 2.5$ and 4° at $z = 0.8$. See Table 1 for some specifics. Along the line of sight, at redshift 0.8 (800 MHz) the BAO scale corresponds to a correlation at 20MHz separation, and at redshift 2.5 (400 MHz), it corresponds to a 12MHz separation correlation. Here we anticipate ~ 5 arcmin or more specifically $5h^{-1}$ Mpc-sized pixels as a standard and thus have very many samples.

2.5 Foregrounds - Galactic and Extragalactic

There are a number of the foregrounds and their possible values:

1) The CMB has a flat antenna temperature of about 2.72 K for the frequencies of interest here. This is not a concern here except for the added noise and the need for the HI emitters to be at a different temperature. The variations of the CMB at

Redshift z	Angle 10 Mpc (arcmin)	Angle 10 h^{-1} Mpc (arcmin)	Angle 150 h^{-1} Mpc (degree)
0.5	26.56'	26'	6.5°
1	20.3'	14.9'	3.72°
2	19.2'	9.5'	2.38°
3	21.1'	7.75'	1.94°
4	23.4'	6.87'	1.72°
5	25.9'	6.34'	1.59°

Table 1. Angular Size for two critical comoving sizes: 10 h^{-1} Mpc and the BAO 150 h^{-1} Mpc. Note that since they are expanding, the angle does not stay relatively constant as it does for the simple fixed physical distance of 10 Mpc. The comoving angle goes to relatively constant value at higher redshift. The cosmology assumed here is a flat universe with $\Omega_m = 0.3036$ and $H_0 = 68.34$ km/s/Mpc

the dipole level of 3.6 mK can easily be modelled and the higher order anisotropies are down at the 30 μ K level and not an issue for this proposed experiment until incredible upgrades.

2) Atmospheric Background has, at 1.42 GHz, a typical antenna temperature of about 2 K looking to the zenith. The signal generally decreases as the frequency squared and is thus less important for $z = 1$ by a factor of 4. The issue is the small variation and factors like precipitation and mist or dew. One can be more careful and treat the atmosphere with Lorentzian line shapes or relevant sum of resonances.

3) The major foreground is galactic synchrotron emission and a bit on the galactic plane, mostly HII thermal emission. We can approximate the signal from the galactic synchrotron as $T_{A \text{ synchrotron}} \sim (1 - 6) \times (\nu/1 \text{ GHz})^{-2.7}$ K, the range going from the north galactic pole down to 10 degrees within the plane of the galaxy.

We can convert this to thinking in redshift $T_{A \text{ synchrotron}} \sim (1 - 6) \times (1 + z)^{2.7}$ K. Thus, at very low redshifts the galactic synchrotron is roughly 10^3 to 10^4 brighter than the largest signal we expect and 10^4 to 10^5 times the signal level we hope to observe. At a redshift of $z = 1$, that would be 5 times worse, and for $z = 2$, it would be 16 times worse. Thus we have to think about how to model and remove this serious foreground.

Galactic synchrotron emission is radiation produced by high energy cosmic-ray electrons above a few MeV spiralling in the galactic magnetic field (e.g. [23, 24, 46]). There is lower emission in relatively smooth regions away from the galactic plane and galactic loops. Based upon the synchrotron mechanism one anticipates a running power-law in frequency for the galactic synchrotron brightness temperature:

$$T_{\text{syn}} = A_{\text{syn}} \left(\frac{\nu}{\nu_*} \right)^{-\beta_{\text{syn}} - \Delta\beta_{\text{syn}} \log(\nu/\nu_*)}, \quad (2.8)$$

where A_{syn} is synchrotron brightness temperature at $\nu_* = 1$ GHz, and β_{syn} and $\Delta\beta_{\text{syn}}$ are the spectral index and spectral running index, respectively. From the 408 MHz

all-sky continuum survey of ref [35, 36], Haverkorn, Katgert and de Bruyn[37] estimated the mean brightness temperature at 408 MHz to be ~ 33 K with temperature uncertainty of $\sim 10\%$. There is some uncertainty in the zero point of the map. After subtraction of the ~ 2.7 K contribution of the CMB and the ~ 3.1 K contribution of extragalactic sources (e.g. [31, 41?]), the diffuse synchrotron galactic background is ~ 27.2 K at 408 MHz. For a spectral index of 2.74 [47] the estimated synchrotron brightness temperature at 1 GHz would be $A_{\text{syn}} = 2.4 \pm 0.24$ K. At high galactic latitudes, the brightness temperature has a minimum of ~ 1 K [41, 51?]. A larger range of estimates for the mean spectral index range from 2.6 to 2.8 (e.g. [23, 24, 31, 41, 47, 52, 54?] with indications for dispersion at each position on the sky, due to distinct components along the line-of-sight (e.g. [23, 24, 41, 51?]). For estimation purposes we choose a typical spectral index of $\beta_{\text{syn}} = 2.7$ with dispersion of 0.1 [51?], and spectral running index of $\Delta\beta_{\text{syn}} = 0.1$ [52, 53]. Kogut[40] has done a careful analysis of the synchrotron spectral index and fits it with an index $\beta_{\text{syn}} = 2.6$ and $\Delta\beta_{\text{syn}} = 0.06$. There is clearly an allowed range so in practice we will use a number in the 2.6 to 2.7 range with some sort of weighted prior.

4) Free-free thermal emission comes from ionized regions in the interstellar medium (ISM), with electron temperature of $T_e > 8000$ K. Again, the physical mechanism for free-free emission imply a good approximation is a running power-law in frequency for the galactic free-free brightness temperature [53],

$$T_{\text{ff}} = A_{\text{ff}} \left(\frac{\nu}{\nu_*} \right)^{-\beta_{\text{ff}} - \Delta\beta_{\text{ff}} \log(\nu/\nu_*)}, \quad (2.9)$$

where A_{ff} is the free-free brightness temperature at $\nu_* = 1$ GHz, and β_{ff} and $\Delta\beta_{\text{ff}}$ are the spectral index and spectral running index, respectively. One can estimate $A_{\text{ff}} = 0.12 \pm 0.01$ K assuming 10% temperature uncertainty. At high frequencies ($\nu > 10$ GHz) the brightness temperature spectral index is $\beta_{\text{ff}} = 2.15$, while at low frequencies it drops to $\beta_{\text{ff}} = -2.0$ due to optically thick self-absorption [26]. Since the gas is optically thin above a few MHz, the brightness temperature spectrum is well described with a spectral index of $\beta_{\text{ff}} = 2.10 \pm 0.01$ [51], and the spectral running index is $\Delta\beta_{\text{ff}} = 0.01$ [52, 53].

5) Extragalactic radio sources - The survey should use existing maps of radio sources and its own ability to discriminate point sources to block out those pixels containing them. There is a reasonable argument that the confusion limit will be handled by the large beam size and power spectrum treatment and exclusion.

The total emission of extragalactic foregrounds has been estimated both directly and from integrated source counts. At 150 MHz, its contribution to the contamination varies from ~ 30 K [32, 54] to ~ 50 K [31, 41?]. At 1 GHz (midway between $z = 0$ and $z = 1$), the estimate is roughly 0.15 K. These foregrounds produce $\sim 10\%$ of the total contamination on average, but can reach $\sim 25\%$ at high galactic latitudes, at the minimum brightness temperature of the diffuse galactic emission.

Most foregrounds are due to radio point sources and relate to active galactic nuclei (AGN) activity. Radio haloes and radio relics are also significant foregrounds, but since they appear only in rich galaxy clusters, they are rare. The remaining extragalactic

foregrounds, which are also the less significant ones, are synchrotron and free-free emission from star forming galaxies, and free-free emission from ionized hydrogen dark matter haloes and diffuse IGM.

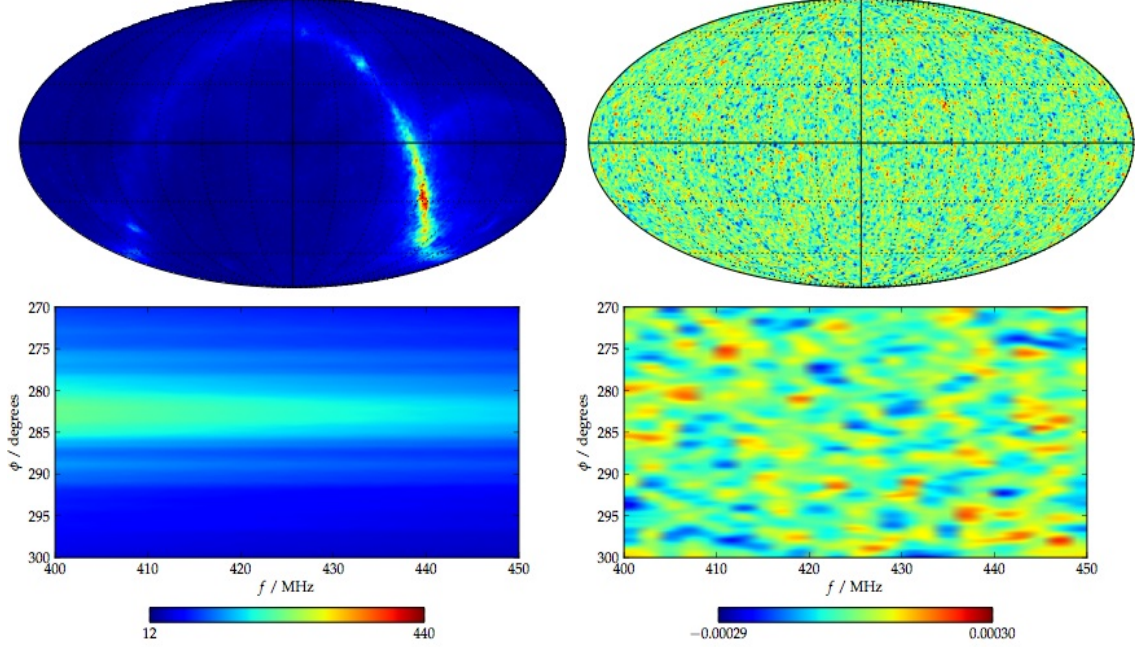


Figure 3. Figures showing on the right the foregrounds at 400 - 450 MHz and on the left the 21-cm signal for the same frequency range. Figures from reference[8].

2.6 Removal of Foregrounds

There is an extensive literature on the removal of foregrounds from 21-cm intensity mapping. Most of it is focused on the epoch or reionization around redshift 8 - 10. We argue here that the real science gain in general and for FAST in particular, is 21-cm intensity mapping in the range $0.5 < z < 2.5$, where the foreground emission is significantly lower and easier to understand.

The usual discussion of how to treat the diffuse galactic foregrounds is that the synchrotron, radio sources and HII emissions are very smooth in frequency. The 21-cm signal we seek varies rapidly with frequency and that is the signal about which we care. Thus we fit a smooth background composed of

$$T_{foreground} = T_{CMB} + T_{atm}\nu^2 + T_{syn}\nu^{-(2.7+\delta\beta_{syn})} + T_{ff}\nu^{-2.1} + T_{exgal}\nu^{-2.7} + \text{baseline polynomial.} \quad (2.10)$$

Each of these can be fitted with a slightly varying index as we are not concerned with dividing the background into components as much as separating it from our desired signal. One makes a frequency dependence fit to each stack of pixels at a given direction on the sky and then produces a cleaned pixel stack as one is fitting over the redshift-direction. One simply removes the baseline and is left with a differential temperature

map of the anticipated 21-cm signal. In the fitting one can add the priors on the expected level of signal and likely simply include the extragalactic signal as a portion of the synchrotron and the free-free emission reducing the number of parameters for which to fit.

Another approach is to do the 3-D Fourier transform, and collapse the transverse directions on the sky and plot k_{\perp} versus k_{\parallel} amplitudes and then stamp out the galaxy as being all at very low k .

The issue in the foreground removal is that one loses a bit of the very largest scale power in the z-direction if one is not really careful. There is typically around 700 data points in the redshift direction and thus one has 700 pixel values plus about 8 parameters to determine leaving one with a bit of freedom and a reduction in power of the desired signal on the scales of the allowed degrees of freedom. This can be improved upon by doing a combined fit in 3 dimensions and allowing only the 21-cm signal and the extragalactic sources to vary on the small scales and requiring the other sources: CMB, atmosphere, synchrotron, free free to vary only slowly in the transverse directions. For the atmosphere one really needs a monitor or atmospheric emission estimation system. The correlation system with larger angle vertical antenna can provide that information but one can also look for correlations in the the receiver array complex and other indicators. Likewise, regular calibrations or scans across various sources can provide information on the allowed baseline shapes and changes with time or position.

In general there are the signals that do not change much with frequency including the CMB, receiver noise etc. and those with a fairly strong frequency dependence. These signal totals run on the scale of 30 K and we are looking to get down to the 1 mK level and thus need to make the subtraction or removal at the 10^{-4} or better level. One only has reasonable hope when one looks at the power spectrum in angle and particularly in frequency that this might be possible.

The foregrounds must be removed to a part in 10,000 to be below the thermal noise in the maps and to achieve the primary science goals. This will require a careful determination of the absolute calibration and of the beams as a smooth function of frequency.

A more serious discussion on how to make this work and how it will depend upon angular scale etc. and which approaches one might use to see that more than one approach gives the same results. One needs a more detailed description of the instrument and the observation strategy, conditions, etc. in order to make a more precise estimate on how well it can be done.

3 Survey Parameters

3.1 Survey 1: Proof of Concept 2-D Map

One can consider the result of a continuous drift scan. That is, point the FAST beams close to vertical and let the Earth's rotation sweep the beam across the sky at a rate of 15° /hour. Observations made and the data are binned by angle on the sky and by

frequency. Assume we bin on the scale of $5h^{-1}$ Mpc comoving scale in angle and 0.1% in frequency giving roughly the same smooth size pixels in both dimensions. After a few days of scanning what would the slice of data appear as? Figure 4 shows a slice in

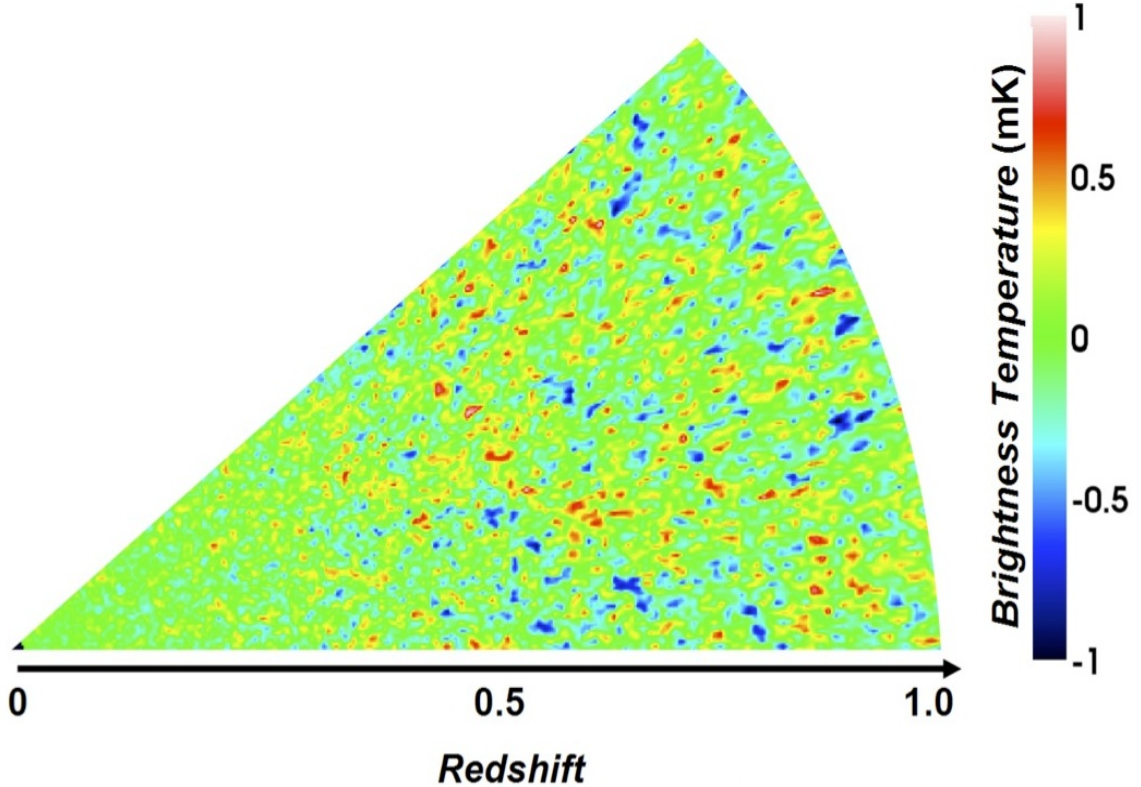


Figure 4. Simulated fluctuations in the brightness temperature of 21-cm emission from galaxies in a slice of the universe. The emission is smoothed over an $8h^{-1}$ Mpc scale. The redshift z and frequency of observation are related by $f = 1.42\text{GHz}/(1+z)$. Red indicates over density and blue under density. Figure from reference[2].

redshift and one angle of the three-dimensional map one would make using 21-cm rest frame intensity map. The frequency range for this map is shown for 0.71 to 1.42 GHz. This simulation assumes a simple power law of perturbations with random phase. This is the kind of map that one might make with a set of drift scans looking at the zenith or near it. With the suggested receiver set for FAST, one could expect to make such a 2-D map with a bit of depth (5 to 10 pixels) to a sensitivity or SNR of 1 to 2 with about two weeks of scanning and serious effort at data processing and analysis to remove the foreground contamination. Such a map would provide a strong proof of concept and produce science results on the BAO scale and larger.

The map would be larger than shown here, extending to 90° in angle and for $0.5 < z < 2.5$. But the ultimate map would depend upon how stable the system is and if data can be taken during daylight hours as well as at night.

Even with this simple but deep Survey 1, there are significant scientific results.

FAST1 could measure both the large scale perturbation spectrum and the BAO peaks fairly accurately over an extended redshift range. E.g., See Figures 5 and 6.

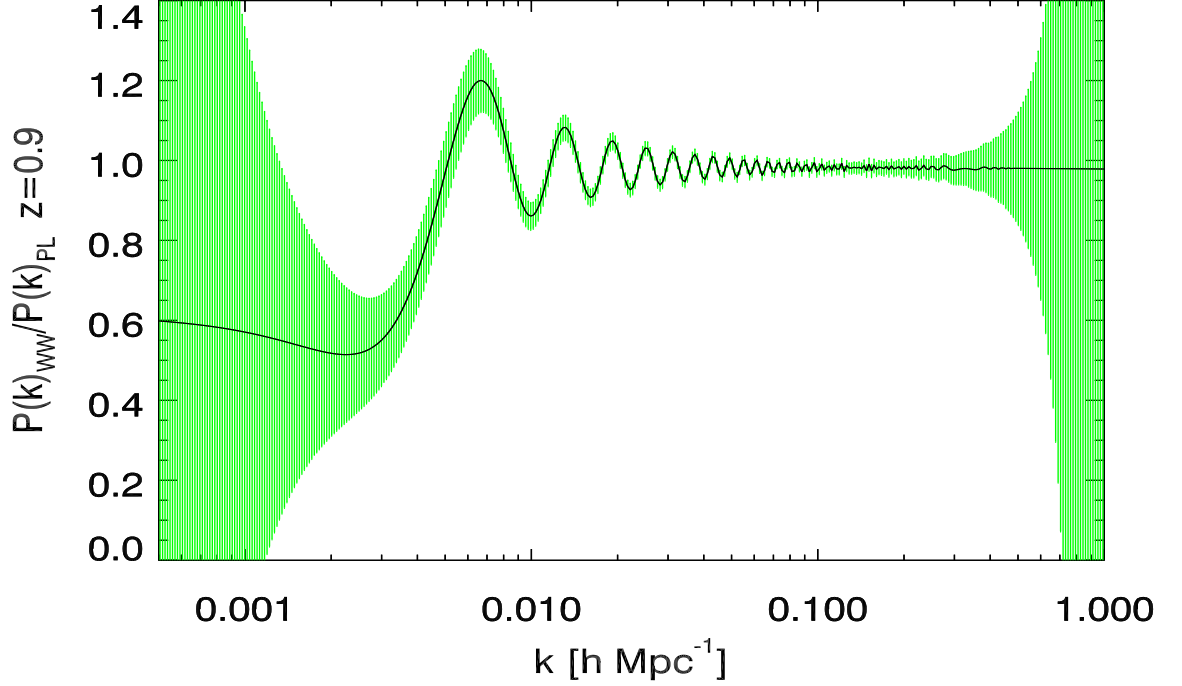


Figure 5. Large scale perturbation power spectrum with error bars for Survey 1 - basically 2-D 21-cm intensity map.

3.2 Survey 2: Large Scale 3-D Perturbation Mapping

It is straight forward but time consuming to move to 3-D perturbation mapping. One simply changes the angle to the zenith in the north-south direction and the earth's rotation provides another slice. It speed things up substantially to have a N-S linear array or receivers in the receiver cabin providing several sections per daily rotation. For reasons of space and preventing cross-talk, the receivers' feeds are likely offset so that one would have to interleave at least a pair of scans to get a completed swath. If the linear array were as large as 10 receivers in the N-S direction, the aberration would not be too severe for the $\pm 5 \times 5 = \pm 25$ arcmin even though FAST is a very fast telescope f-number of about 0.5. To get a swath 40° wide would take about $N = 40^\circ / (n \times 5 \text{ arcmin}) = 48$ (10/n) days, where n is the number of receivers in the N-S direction. Again, one would want to do a detailed concept layout to determine if a 2 by 10 array or something like a 5 by 5 array would produce better performance for FAST as its surface is actively deformed to produce a parabola for the direction of observation.

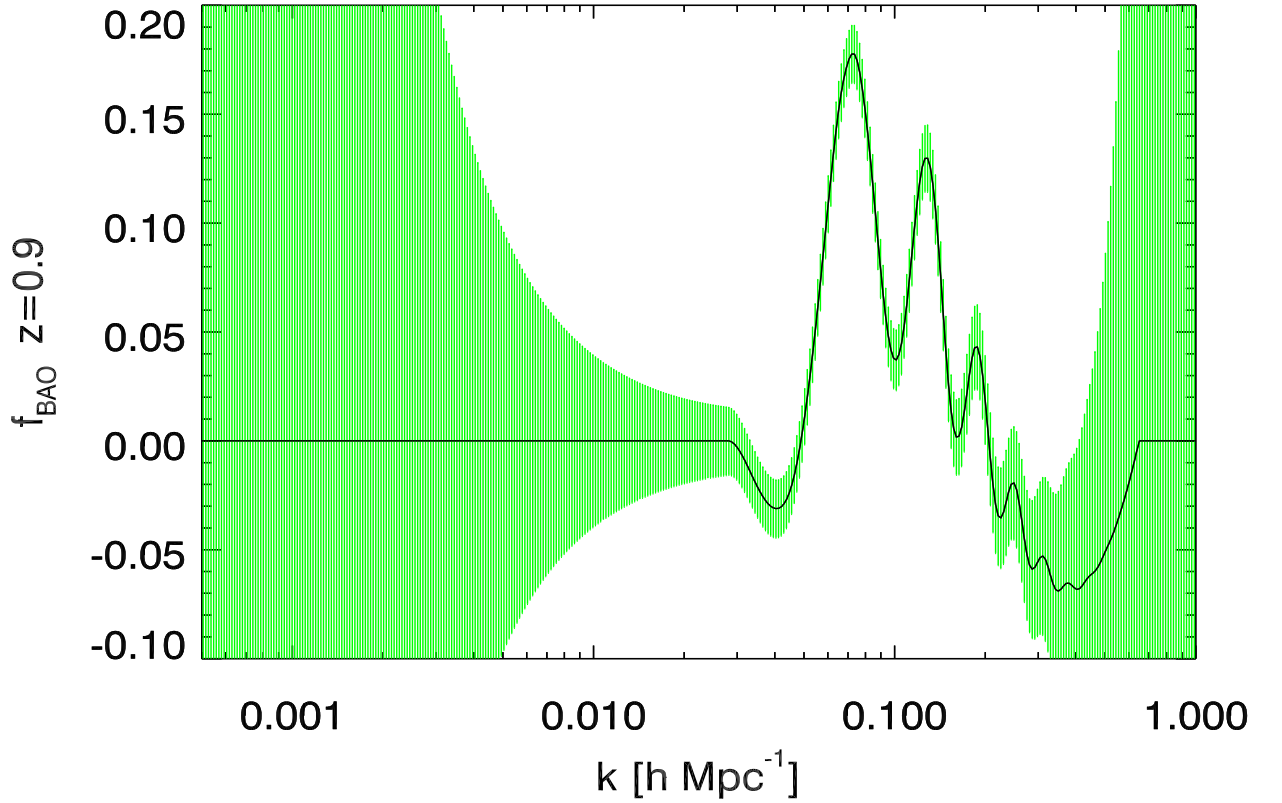


Figure 6. Focus on BAO features perturbation power spectrum with error bars for Survey 1 - basically 2-D 21-cm intensity map. f_{BAO} is the ratio of the processed with BAO power spectrum to a power-law spectrum plus simple power law cut off for the processing suppression. f_{BAO} is forced to 0 outside the k range of interest so as not to consider the likely possible low k perturbations and the more non-linear effects at large k .

Figures 7 and 8 show the kind of performance one might expect for the initial 3-D scan and an extensive 2-year observing program.

4 Anticipated Science

Most of the cosmology science comes from measuring the perturbations - map and power spectrum - and comparing to theoretical predictions and expectations or finding parameter of the models. Thus the precision to which one can make the real space map and determine the perturbation power spectrum determine the reach of the experimental observations.

Figure 9 shows the fractional errors for the two surveys versus wave number k . The two plots are for Survey 1 and Survey 2 parameters. Since the observations are sensitivity limited the errors go down linearly with inverse of the the observing time but only with the inverse of the survey volume which sets the sample variance. Thus since for short observing times the noise variance dominates, the much longer exposure

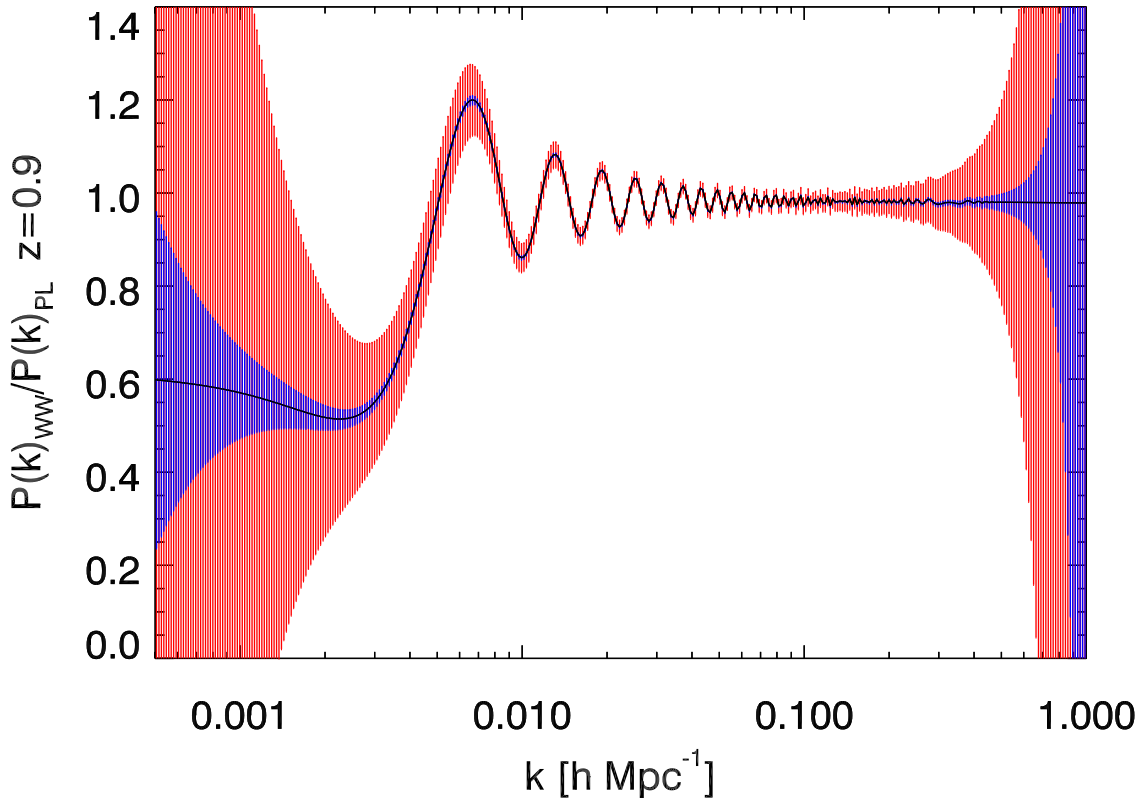


Figure 7. Large scale perturbation power spectrum with error bars for Survey 2, the 3-D 21-cm intensity map. There are two sets of error bars. The large is for the first about 50 day survey. The inner smaller errors are for an effective two-year survey.

time of the Survey 1 per pixel makes up for the longer total exposure (but 14 times shorter per pixel) spread over a much larger volume and thus number of pixels. The 80 times larger volume does not quite make up for the 14 times less integration time per pixel. Survey 1 was chosen to reach about unity in the second term added to one, so it can only improve marginally with more observing time. (It would improve by 25% for about double the proposed 2 week run, compared the more rapid return to 14 days.) While Survey 2 will reduce its fractional error with the inverse of the observing time in units of the base observing time. Thus if Survey 2 is going well and integrating down properly, then it reaches diminishing returns in about 14 times the original mapping time. We also need to allow for the case of the effective system temperature being higher than 20 K or different scan and differencing/foreground removal strategy.

Comparison of Surveys: It is relevant to compare the possible FAST surveys with other proposed surveys. Figure 10 shows the nominal quoted in various publications the fractional sensitivity of various proposed surveys. This comparison is not easy to make as all the different proposed surveys quote their sensitivity in different binnings. Thus we include another more limited comparison in Figure 11 where the FAST surveys have simple $|Deltak = k$ bins and the special Figure 12, which has everything with the

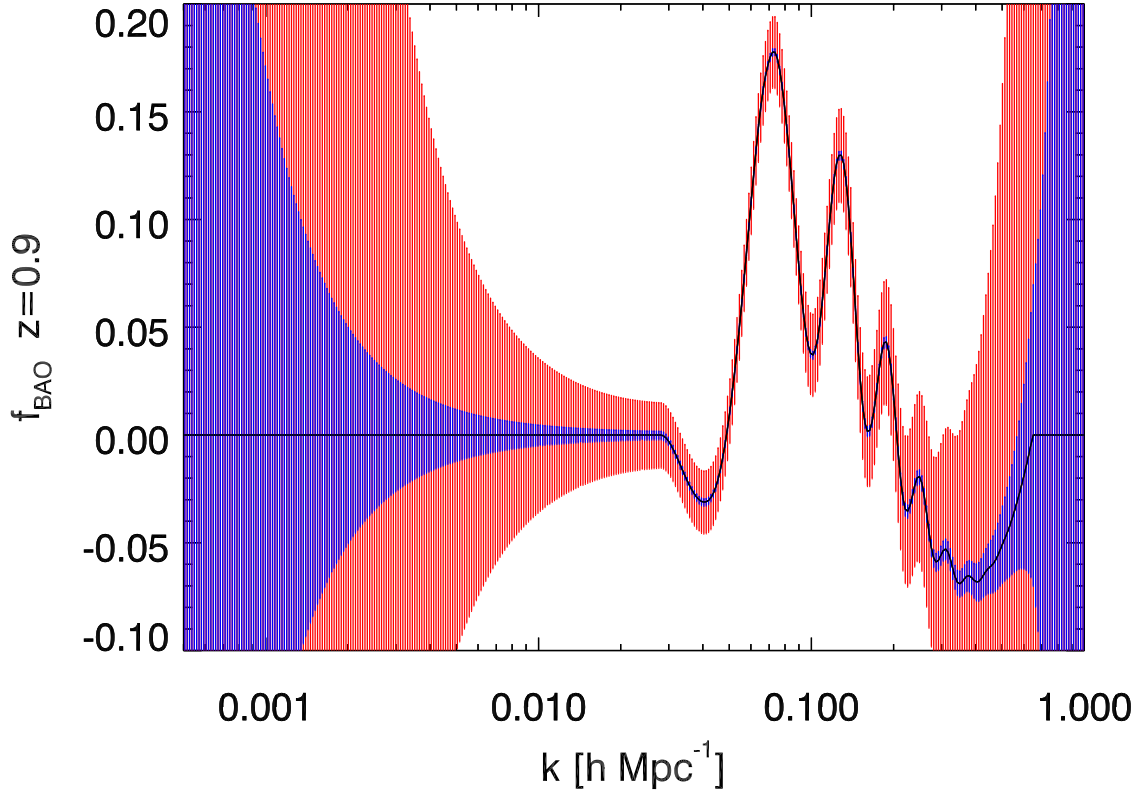


Figure 8. Focus on BAO features perturbation power spectrum with error bars for Survey 2. the 3-D 21-cm intensity map. The outer (red) errors are for the nominal 48-day observing first pass. The inner (blue) error band is for a 2-year observing run assuming that the data integrate down and full sensitivity is achieved and thus the errors on the power spectrum decrease inversely with observing time. f_{BAO} is the ratio of the processed with BAO power spectrum to a power-law spectrum plus simple power law cut off for the processing suppression. f_{BAO} is forced to 0 outside the k range of interest so as not to consider the likely possible low k perturbations and the more non-linear effects at large k .

same 20 bins per decade kindly provided by Philip Bull[18].

4.1 Anticipated Science: Motivated models of large-scale perturbations

In the concordance model of cosmology, the growth of structure is seeded by primordial quantum perturbations which depend on some inflationary potential. To this point the model has used the slow-roll potential model, where the primordial power spectrum model is parametrized by a power law of the form:

$$P_S^{\text{Plaw}}(k) = A_s \left(\frac{k}{k_0} \right)^{n_s-1}, \quad (4.1)$$

where A_s is the normalisation, k_0 is the pivot scale and n_s is the tilt. The latter is $n_s = 1$ for a scale-independent spectrum.

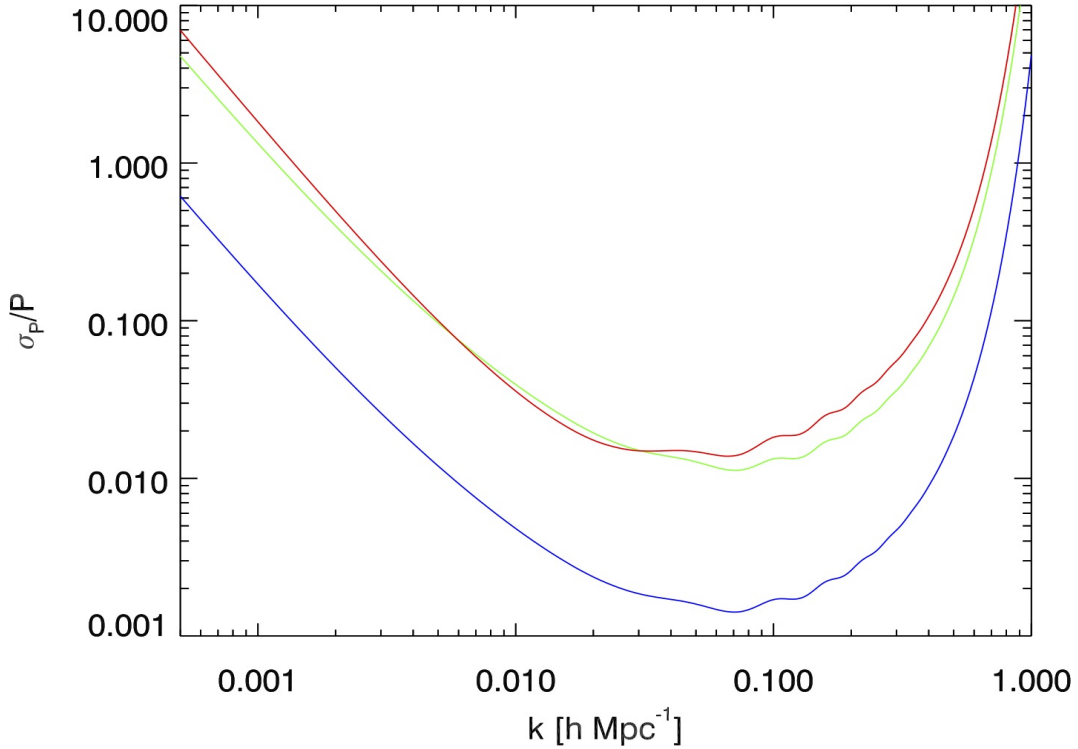


Figure 9. Plot shows the fractional error in the power spectrum versus wave number k at an effective redshift of about $z = 0.9$. The two upper curves are for Survey 1 and Survey 2 parameters, with only a first pass for Survey 2. Since the observations are sensitivity limited the errors go down linearly with inverse of the observing time but only with the inverse square root of the survey volume and the first cut of each gives about the same errors. Thus since for short observing times the noise variance dominates, the much longer exposure time of the Survey 1 makes up for the longer total exposure (but 14 times shorter per pixel) spread over a much larger volume and thus number of pixels. The 80 times larger volume does not quite make up for the 14 times less integration time per pixel. Survey 1 was chosen to reach about unity in the second term added to one at the power spectrum peak, so it can only improve marginally there with more observing time. (It would improve by 25% for about double the proposed 2 week run, compared the more rapid return to 14 days. It does improve away from the power spectrum peak still.) While Survey 2 will reduce its fractional error with the inverse of the observing time in units of the base observing time. Thus if Survey 2 is going well and integrating down properly, then it reaches diminishing returns in about 14 times the original mapping time. The lower curve shows the fractional error that would be achievable with two years of observations in Survey 2 mode assuming an $> 80\%$ duty cycle. We also need to allow for the case of the effective system temperature being higher than 20 K or different scan and differencing/foreground removal strategy.

The most remarkable result to come out of the Planck mission so far is the 5σ tension between the data and the scale-independent primordial power spectrum model

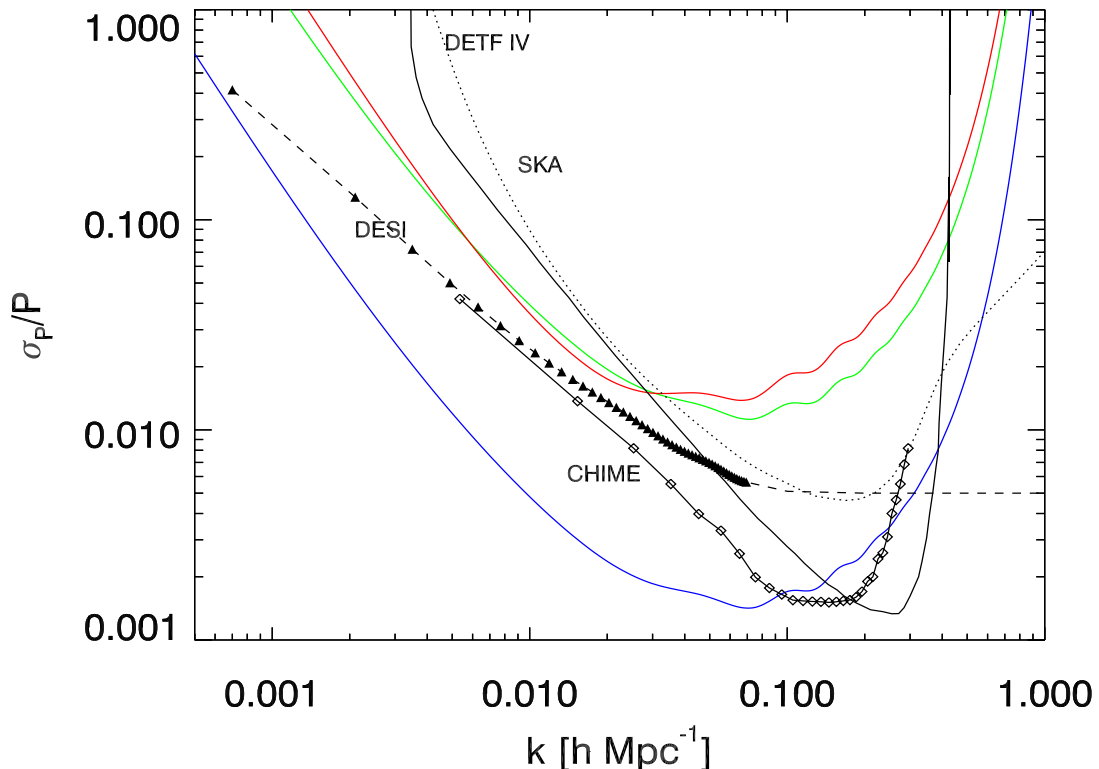


Figure 10. Comparison of surveys. Plot shows the fractional error in the power spectrum versus wave number k at an effective redshift of about $z = 0.9$ for the FAST surveys as in the previous figure. Additional points and curves are for other experiments including the DESI[22] galaxy and quasar/Lyman-alpha survey and CHIME[8] 21-cm Intensity Mapping survey. The DESI points are truncated to 0.5% error for the small scales or larger k as a rough estimate of potential systematic effects, which are essentially neglected in the other surveys at this point. The DETF IV (Dark Energy Task Force stage IV) outline of fractional error. DETF IV aims specifically at measuring the BAO features very accurately to test Dark Energy effects but neglects to consider the importance of testing the very high energy effects of Inflation. Specifically, looking at the horizon scale at recombination and above where the effects of early Inflation and early universe phase transitions are most likely to be manifested. These plots are not a direct comparison in that different experiments used different binning in k

[10]. This strengthens and verifies the observed ‘low power at large scales’ anomaly first observed by COBE[56] and then strengthened by the WMAP results[57].

Those observations leads us to conclude that the primordial power spectrum is scale-dependent. The recent claim by the BICEP2 team [9] of the detection of primordial gravitational waves has reopened the crucial question of inflation, motivating the proposition of various models. The Wiggly Whipped Inflation model[12], seems to fit joint Planck and BICEP-2 data (particularly the deviation from a smooth pri-

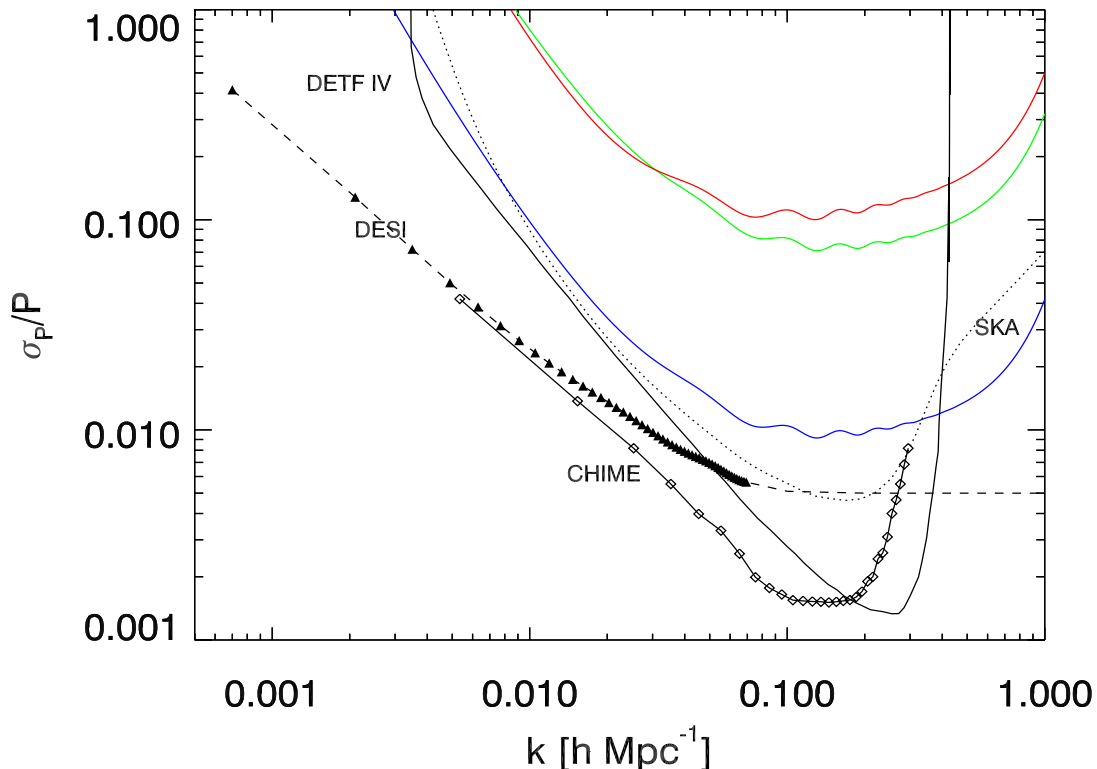


Figure 11. A slightly different comparison of surveys with different Δk binning for the FAST surveys. Plot shows the fractional error in the power spectrum versus wave number k at an effective redshift of about $z = 0.9$ for the FAST surveys as in the previous figure. This plot has the same curves but with FAST binned in $\Delta k = k$ bins. The SKA bins are one per cent bins. While the CHIME bins are in very broad bins chosen to sample the baryon oscillations roughly.

mordial power spectrum) better than other models. These fall in the general class of just enough inflation[58] models, which generically produce suppression of power on the largest angular scales and an oscillatory behaviour at scales around the Hubble parameter at the beginning of the slow roll inflation that covers most of the observations of CMB and large scale structure.

The primordial power spectrum resulting from this model leaves an imprint on large-scale structure at the present epoch. More importantly, it may show features at scale which can be probed by weak lensing surveys such as the future Euclid mission.

One version of the ‘Wiggly Whipped’ Inflation potential has the form

$$V(\phi) = \gamma\phi^2 + \lambda\phi^2(\phi - \phi_0)\Theta(\phi - \phi_0) \quad (4.2)$$

where Θ is a Heavyside step function modified to be the smooth $\Theta(\phi - \phi_0) = 1 + \tanh((\phi - \phi_0)/\Delta\phi)$, $\Delta\phi$ is constant indicating the smoothness of the step and ϕ_0 is the transition point of the inflaton field.

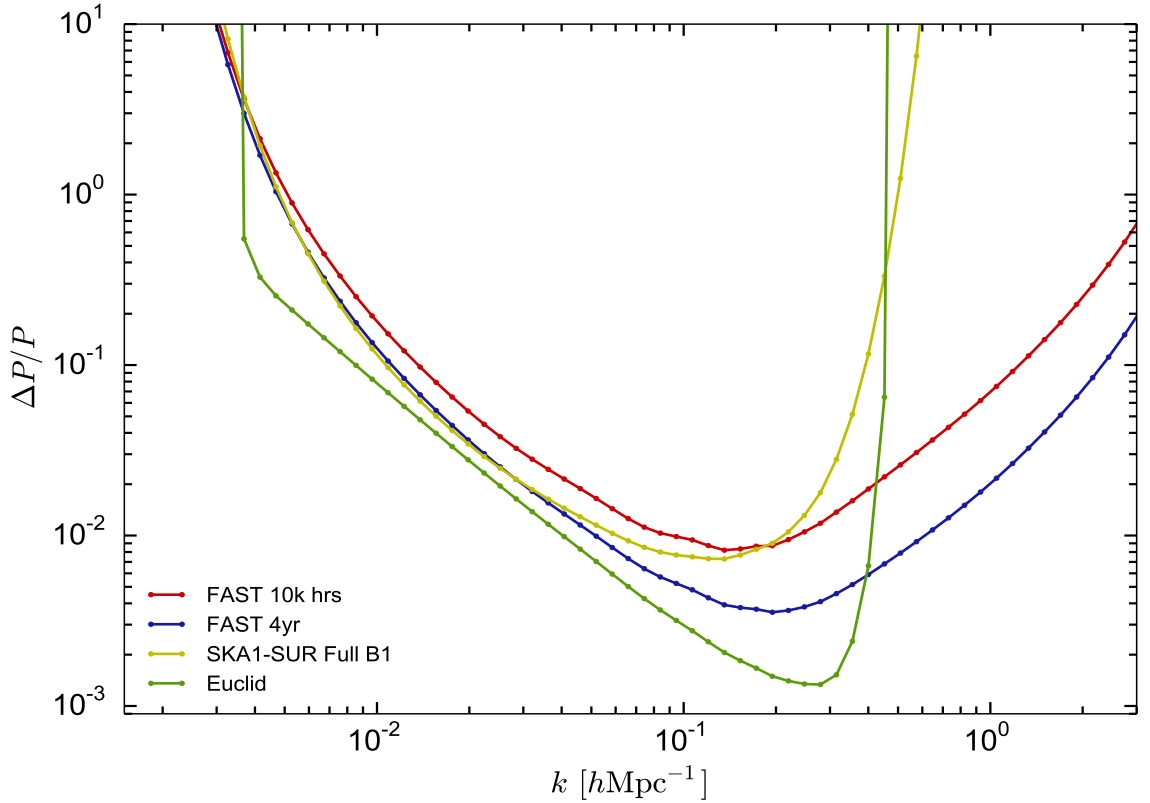


Figure 12. Yet another comparison of surveys all with Δk binning of 20 per decade and sky coverage of about 25 000 square degrees. Plot shows the fractional error in the power spectrum versus wave number k and shows that FAST and SKA1 survey are more directly comparable. The curve labeled Euclid effectively represents cosmic variance-limited observations over a similar redshift range and is basically the DETF IV curve on the previous plots. This shows that the two programs can approach cosmic variance limits in the central k range but begin to suffer from signal-to-noise limitations at low $k < 10^{-2} h\text{Mpc}^{-1}$ and $k > 0.2 h\text{Mpc}^{-1}$. This plot provided by Philip Bull[18].

In order to measure the features in the matter power spectrum which would be imprinted by this inflation potential, we need to look for any deviations from a power-law fit to the data. We therefore consider the ratio of the power spectra given by Wiggly Whipped Inflation and the simplest power law inflation.

We calculate the full nonlinear matter power spectrum $P(k)$ using the publicly available Boltzmann code CAMB [13], taking the *Planck* best fitting values for our fiducial cosmology: $h = 0.7$, $\Omega_\Lambda = 0.7$, $w = -1$, $\Omega_m = 0.3$, $\Omega_b = 0.0462$, $\tau = 0.09$, $N_{\text{eff}} = 3.046$. The Wiggly Whipped Inflation potential is calculated using BINGO [11].

In Figure 13, we show the errors on this ratio given by the FAST survey considered in this paper for the particular model Wiggly Whipped Inflation[12]. It is important to

emphasize here that generally models with just enough Inflation (50 to 60 e-folds) will generally show features in the regime $0.0001 < k < 0.002$ and then wiggles beginning around $k \sim 0.002 \text{ Mpc}^{-1}$ and damping to larger k . Observations bias the low k features to on average be a dip.

4.2 Anticipated Science: Observing BAO features

Clear basic science for the FAST 21-cm intensity mapping is observing that BAO features and using them to determine cosmological parameters and comparison to other survey techniques including galaxy and weak lensing surveys

Measuring the BAO features with accuracy and precision and more than one technique make it possible to probe the nature of Dark Energy (the acceleration of the universe), large scale structure formation, Dark Matter effects and properties, and to test alternate theories of gravity. As shown here and the two previous BAO figures, the FAST 21-cm intensity mapping has the potential to measure these features well in the critical and scientifically powerful redshift range from $0.5 < z < 2.5$. There is the potential to extend and improve these maps should the scientific results warrant.

4.3 Anticipated Science: Testing General Relativity

With sufficient observations it is possible to test General Relativity on the large scale with FAST observations via 21-cm intensity mapping[21]. Combined with systematic pulsar observations one can have a serious suite of tests of General Relativity.

4.4 Anticipated Ancillary Science:

4.4.1 Radio Transients:

Because of the unprecedented combination of a large collecting area, good angular resolution, and 24 hour operation, FAST will detect and monitor thousands of previously unknown transient sources. The bulk of radio transients which have been discovered to date have been found using the Parkes Multi-beam survey (11 so far). Because of the small number of sources thus far observed, the luminosity function is very poorly constrained, so precise projections of the detection rate are not possible. FAST observations will go much deeper than the Parkes survey. If both CHIME and the FAST 21-cm survey are underway at the same time, then sharing catalogs and observations of these sources will make both surveys more productive in this effort. CHIME has the advantage that it is scanning a large celestial latitude band simultaneously providing more coverage and detection rate, while FAST has the advantage of a larger collecting area and thus signal-to-noise on these events. The FAST Intensity mapping is a transit mode, once a source is detected the pulse pattern of the source can be searched for, both in the future scans and retrospectively, in each days data. Given the recent success of radio transient searches, it is reasonable to anticipate that completely new types of sources will appear in the FAST observations.

4.4.2 Pulsars:

Because of its large field of view, FAST will provide an capability to time known pulsars, and eventually to search for new ones. FAST also has receivers in many

bands and already a program for pulsar timing and dispersion/de-dispersion treatment. All pulsars in the mostly Northern hemisphere FOV will spend from 5 minutes to hours within the FAST intensity mapping fields of view. From a list of locations and dispersion measures a data set of timing and scintillation for hundreds of pulsars will be produced.

4.4.3 Galactic Magnetic Fields:

GMIMS, the Global Magneto-Ionic Medium Survey. major objective is to improve knowledge and understanding of the Galactic magnetic field. GMIMS will do this by mapping the polarized radio emission from the Milky Way in the frequency band 300 to 1800 MHz. Data in this spectral range will reveal aspects of how magnetic fields regulate star formation and couple the energy released by stellar winds and supernovae to the interstellar medium. FAST, if polarisation information is included, will provide much more sensitive data over the middle part of this frequency band. This might happen in a differential measurement.

5 Conclusions and Future

The potential program outlined here has very strong science products. They point out that FAST has the potential to provide a treasure trove of cosmological observations. There are a number of ways to improve our understanding of the universe and the potential of this instrument and this potential program. The next steps are to refine the survey parameters and observing plan and to provide a full concept and design for the receiver and data processing systems.

Acknowledgements

G.F.S. acknowledges support through his Chaire d’Excellence Université Sorbonne Paris Cité and the financial support of the UnivEarthS Labex program at Université Sorbonne Paris Cité (ANR-10-LABX-0023 and ANR-11-IDEX-0005-02).

References

- [1] Rendong Nan Di Li, Chengjin Jin, Qiming Wang, Lichun Zhu, Wenbai Zhu, Haiyan Zhang, Youling Yue and Lei Qian, arXiv:1105.3794, International Journal of Modern Physics D, “The Five-Hundred-Meter Aperture Spherical Radio Telescope (FAST) Project”
B. Peng, R.G. Strom, R. Nan, E. Ma, J. Ping, L. Zhu, W. Zhu, In Perspectives in Radio Astronomy: Scientific Imperatives at cm and m Wavelengths (Amsterdam: NFRA), Ed. M.P. van Haarlem and J.M. van der Hulst, 1999, 25
Bo Peng, Chengjin Jin, Qiming Wang, Lichun Zhu, Wenbai Zhu, Haiyan Zhang, and Rendong Nan, “Preparatory Study for Constructing FAST, the Worlds Largest Single Dish” Proceedings of the IEEE — Vol. 97, No. 8, August 2009
- [2] Peterson et al., “21 cm Intensity Mapping” arXiv:0902.3091 and references therein.

- [3] Chang, T.-C., Pen, U.-L., Bandura, K., and Peterson, J. B., “An intensity map of hydrogen 21-cm emission at redshift z 0.8,” *Nature* 466, 463465 (July 2010).
Switzer, E. R., Masui, K. W., Bandura, K., Calin, L. M., Chang, T. C., Chen, X. L., Li, Y. C., Liao, Y. W., Natarajan, A., Pen, U.-L., Peterson, J. B., Shaw, J. R., and Voytek, T. C., “Determination of z 0.8 neutral hydrogen Fluctuations using the 21 cm intensity mapping autocorrelation,” *Monthly Notices of the Royal Astronomical Society: Letters*, L125 (June 2013).
Masui, K. W., Switzer, E. R., Banavar, N., Bandura, K., Blake, C., Calin, L. M., Chang, T. C., Chen, X., Li, Y. C., Liao, Y. W., Natarajan, A., Pen, U.-L., Peterson, J. B., Shaw, J. R., and Voytek, T. C., “Measurement of 21 cm Brightness Fluctuations at $z = 0.8$ in Cross-correlation,” *The Astrophysical Journal Letters* 763, L20 (Jan. 2013).
- [4] Stefano Camera, Mario G. Santos, Pedro G. Ferreira, and Lus Ferramacho, arXiv:1305.6928 “Cosmology on Ultralarge Scales with Intensity Mapping of the Neutral Hydrogen 21 cm Emission: Limits on Primordial Non-Gaussianity”
- [5] A. R. Liddle, *An Introduction to Cosmological Inflation*, in *High Energy Physics and Cosmology, 1998 Summer School* (A. Masiero, G. Senjanovic, and A. Smirnov, eds.), p. 260, 1999. [astro-ph/9901124](#).
- [6] These two images are scanned from NASA SP-419, “The Search for Extraterrestrial Intelligence”, as reprinted on page 42-43 of the Dover edition, ISBN 0-486-23890-3
- [7] <http://ned.ipac.caltech.edu/level5/March02/Sahni/Sahni4-5.html>
- [8] CHIME: Canadian Hydrogen Intensity Mapping Experiment, <http://chime.phas.ubc.ca/VanderLinde2013/cifar.pdf>
- [9] P. A. R. Ade, R. W. Aikin, D. Barkats, S. J. Benton, C. A. Bischoff, J. J. Bock, J. A. Brevik, I. Buder, E. Bullock, C. D. Dowell, L. Duband, J. P. Filippini, S. Fliescher, S. R. Golwala, M. Halpern, M. Hasselfield, S. R. Hildebrandt, G. C. Hilton, V. V. Hristov, K. D. Irwin, K. S. Karkare, J. P. Kaufman, B. G. Keating, S. A. Kernasovskiy, J. M. Kovac, C. L. Kuo, E. M. Leitch, M. Lueker, P. Mason, C. B. Netterfield, H. T. Nguyen, R. O’Brien, R. W. Ogburn, A. Orlando, C. Pryke, C. D. Reintsema, S. Richter, R. Schwarz, C. D. Sheehy, Z. K. Staniszewski, R. V. Sudiwala, G. P. Teply, J. E. Tolan, A. D. Turner, A. G. Vieregg, C. L. Wong, K. W. Yoon, and Bicep2 Collaboration, *Detection of B-Mode Polarization at Degree Angular Scales by BICEP2*, *Physical Review Letters* **112** (June, 2014) 241101, [[arXiv:1403.3985](#)].
- [10] Planck Collaboration, *Planck 2013 results. XVI. Cosmological parameters, A&A*, preprint (arXiv:1303.5076) (Mar., 2013) [[arXiv:1303.5076](#)].
- [11] D. K. Hazra, L. Sriramkumar, and J. Martin, *BINGO: a code for the efficient computation of the scalar bi-spectrum*, *JCAP* **5** (May,2013) 26, [[arXiv:1201.0926](#)].
- [12] D. K. Hazra, A. Shafieloo, G. F. Smoot, and A. A. Starobinsky, *Wiggly Whipped Inflation*, *ArXiv e-prints* (May, 2014) [[arXiv:1405.2012](#)].
- [13] A. Lewis, A. Challinor, and A. Lasenby, *Efficient Computation of Cosmic Microwave Background Anisotropies in Closed Friedmann-Robertson-Walker Models*, *Astrophysical Journal* **538** (Aug., 2000) 473–476, [[astro-ph/](#)].
- [14] M. Tegmark, M. R. Blanton, M. A. Strauss, F. Hoyle, D. Schlegel, R. Scoccimarro, M. S. Vogeley, D. H. Weinberg, I. Zehavi, A. Berlind, T. Budavari, A. Connolly, D. J.

- Eisenstein, D. Finkbeiner, J. A. Frieman, J. E. Gunn, A. J. S. Hamilton, L. Hui, B. Jain, D. Johnston, S. Kent, H. Lin, R. Nakajima, R. C. Nichol, J. P. Ostriker, A. Pope, R. Scranton, U. Seljak, R. K. Sheth, A. Stebbins, A. S. Szalay, I. Szapudi, L. Verde, Y. Xu, J. Annis, N. A. Bahcall, J. Brinkmann, S. Burles, F. J. Castander, I. Csabai, J. Loveday, M. Doi, M. Fukugita, J. R. Gott, III, G. Hennessy, D. W. Hogg, Z. Ivezić, G. R. Knapp, D. Q. Lamb, B. C. Lee, R. H. Lupton, T. A. McKay, P. Kunszt, J. A. Munn, L. O’Connell, J. Peoples, J. R. Pier, M. Richmond, C. Rockosi, D. P. Schneider, C. Stoughton, D. L. Tucker, D. E. Vanden Berk, B. Yanny, D. G. York, and SDSS Collaboration, *The Three-Dimensional Power Spectrum of Galaxies from the Sloan Digital Sky Survey*, *Astrophysical Journal* **606** (May, 2004) 702–740, [[astro-ph/0310725](#)].
- [15] H. Gil-Marín, C. Wagner, L. Verde, C. Porciani, and R. Jimenez, *Perturbation theory approach for the power spectrum: from dark matter in real space to massive haloes in redshift space*, *JCAP* **11** (Nov., 2012) 29, [[arXiv:1209.3771](#)].
- [16] P. J. E. Peebles, *The large-scale structure of the universe*. Princeton Series in Physics, Princeton, NJ, 1980.
- [17] S. J. Maddox, G. Efsthathiou, W. J. Sutherland, and J. Loveday, *Galaxy correlations on large scales*, *Monthly Notices of Royal Astronomical Society* **242** (Jan., 1990) 43P–47P.
- [18] Philip Bull, Pedro G. Ferreira, Prina Patel, Mario G. Santos [arXiv:1405.1452](#) “Late-time cosmology with 21 cm intensity mapping experiments”
- [19] R.A. Battye, M.L. Brown, I.W.A. Browne, R.J. Davis, P. Dewdney, C. Dickinson, G. Heron, B. Maffei, A. Pourtsidou, P.N. Wilkinson [arXiv:1209.1041](#) “BINGO: a single dish approach to 21cm intensity mapping”
- [20] “Projected Constraints on Modified Gravity Cosmologies from 21 cm Intensity Mapping” Kiyoshi Wesley Masui, Fabian Schmidt, Ue-Li Pen, Patrick McDonald [arXiv:0911.3552](#)
- [21] “Testing General Relativity with 21 cm intensity mapping” Alex Hall, Camille Bonvin, Anthony Challinor [arXiv:1212.0728](#)
- [22] Dark Energy Spectroscopic Instrument (DESI) will measure the effect of dark energy on the expansion of the universe. It will obtain optical spectra for tens of millions of galaxies and quasars, <http://desi.lbl.gov> DESI web site etc. and estimated errors via private communication from Pat McDonald.
- [23] Banday A. J., Wolfendale A. W., 1990, *MNRAS*, 245, 182
- [24] Banday A. J., Wolfendale A. W., 1991, *MNRAS*, 248, 705
- [25] Barkana R., Loeb A., 2005, *ApJ*, 624, L65
- [26] Bennett C. L. *et al.*, 2003, *ApJS*, 148, 97
- [27] Benson A. J., Nusser A., Sugiyama N., Lacey C. G., 2001, *MNRAS*, 320, 153
- [28] Benson A. J., Sugiyama N., Nusser A., Lacey C. G., 2006, *MNRAS*, 369, 1055
- [29] Blanton M. R. *et al.*, 2001, *AJ*, 121, 2358
- [30] Blanton M. R. *et al.*, 2003, *ApJ*, 592, 819
- [31] Bridle A. H., 1967, *MNRAS*, 136, 219

- [32] Cane H. V., 1979, MNRAS, 189, 465
- [33] Gnedin N. Y., Shaver P. A., 2004, ApJ, 608, 611
- [34] Liron Gleser, Adi Nusser, Andrew J. Benson “De-contamination of cosmological 21-cm maps” 0712.0497v2
- [35] Haslam C. G. T., Klein U., Salter C. J., Stoffel H., Wilson W. E., Cleary M. N., Cooke D. J., Thomasson P., 1981, A&A, 100, 209
- [36] Haslam C. G. T., Salter C. J., Stoffel H., Wilson, W. E., 1982, A&AS, 47, 1
- [37] Haverkorn M., Katgert P., de Bruyn A. G., 2003, A&A, 403, 1031
- [38] Jelic V. *et al.*, 2008, MNRAS, 389, 1319
- [39] Kempner J. C., Blanton E. L., Clarke T. E., Enßlin T. A., Johnston-Hollitt M., Rudnick L., 2004, in *The Riddle of Cooling Flows in Galaxies and Clusters of Galaxies* Conference Note
- [40] Kogut, A. 1205.4041, “SYNCHROTRON SPECTRAL CURVATURE FROM 22 MHZ TO 23 GHZ”
- [41] Lawson K. D., Mayer C. J., Osborne J. L., Parkinson M. L, 1987, MNRAS, 225, 307
- [42] McQuinn M., Zahn O., Zaldarriaga M., Hernquist L., Furlanetto S. R., 2006, ApJ, 653, 815
- [43] Morales M. F., Hewitt J., 2004, ApJ, 615, 7
- [44] Morales M. F., Bowman J. D., Hewitt J., 2006, ApJ, 648, 767
- [45] Oh S. P., Mack K. J., 2003, MNRAS, 346, 8710
- [46] Pacholczyk A. G., 1970, Radio Astrophysics, Freeman & Co., San Francisco
- [47] Platania P., Burigana C., Maino D., Caserini E., Bersanelli M., Cappellini B., Mennella A., 2003, A&A, 410, 847
- [48] Rybicki G. B., Press W. H., 1992, ApJ, 398, 169
- [49] Rybicki G. B., Lightman A. P., 1979, Radiative Processes in Astrophysics, Wiley, New York
- [50] Santos M. G., Cooray A., Knox L., 2005, ApJ, 625, 575
- [51] Shaver P. A., Windhorst R. A., Madau P., de Bruyn A. G., 1999, A&A, 345, 380
- [52] Tegmark M., Eisenstein D. J., Hu W., de Oliveira-Costa A., 2000, ApJ, 530, 133
- [53] Wang X., Tegmark M., Santos M. G., Knox L., 2006, ApJ, 650, 529
- [54] Willis A. G., Oosterbaan C. E., Lepoole R. S., de Ruiter H. R., Strom R. G., Valentijn E. A., Katgert P., Katgert-Merkelijn J. K., 1977, in Jauncey D. L., ed, IAU Symposium, No. 74, Radio Astronomy and Cosmology, D. Reidel Publishing Co., Holland, p. 39
- [55] Zaldarriaga M., Furlanetto S. R., Hernquist L., 2004, ApJ, 608, 622
- [56] Smoot et al. 1992 Astrophysical Journal vol. 396, no. 1, Sept. 1, 1992, p. L1-L5. J. Bond, A. H. Jaffe, and L. Knox, Estimating the power spectrum of the cosmic microwave background, Phys.Rev. D57 (1998) 21172137, [astro-ph/9708203].

- G. Hinshaw, A. Banday, C. Bennett, K. Gorski, A. Kogut, et al., 2-point correlations in the COBE DMR 4-year anisotropy maps, *Astrophys.J.* 464 (1996) L25L28, [astro-ph/9601061]
- [57] WMAP Collaboration Collaboration, D. Spergel et al., First year Wilkinson Microwave Anisotropy Probe (WMAP) observations: Determination of cosmological parameters, *Astrophys.J.Suppl.* 148 (2003) 175194, [astro-ph/0302209].
- [58] Michele Cicoli, Sean Downes, Bhaskar Dutta, Francisco G. Pedro, Alexander Westphal “Just enough Inflation: power spectrum modications at large scales” arXiv:1407.1048 *MNRAS*, 375, 1269

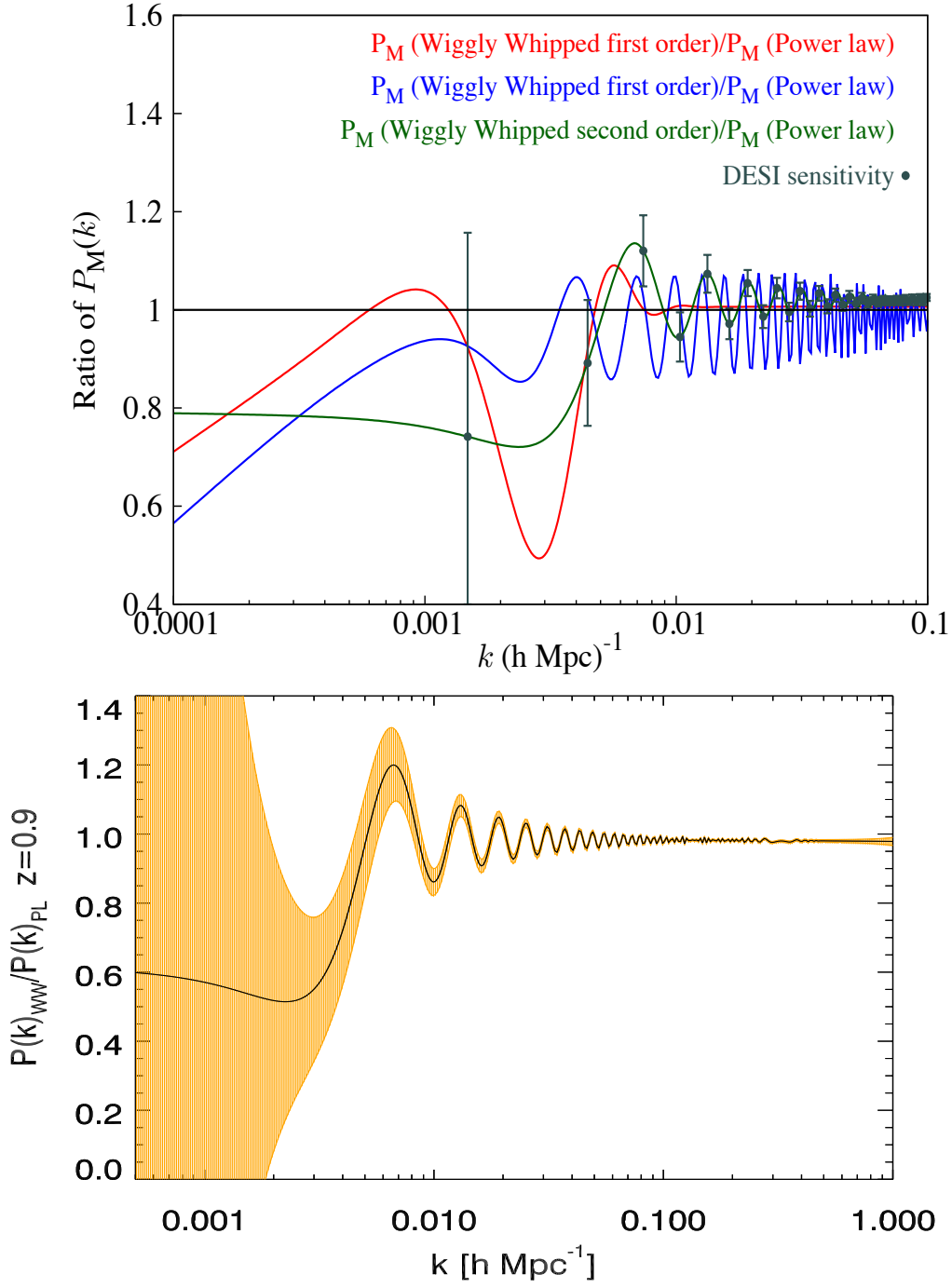


Figure 13. Example of the kind of large scale primordial perturbations one might have for large field inflation affected by the GUT transition or other features. These example have the generic features of ‘just enough’ Inflation (50-60 e-folds). These curves are the best-fitted to CMB data models from Wiggly Whipped Inflation[12] showing the errors for DESI on the particular model shown with the FAST errors in the previous plots. Lower figure is the same curve but with AST 2 year survey continued to 4 years and the sky coverage doubled. Note that 21-cm intensity mapping on large scales is an ideal efficient method to obtain high quality data in this region.

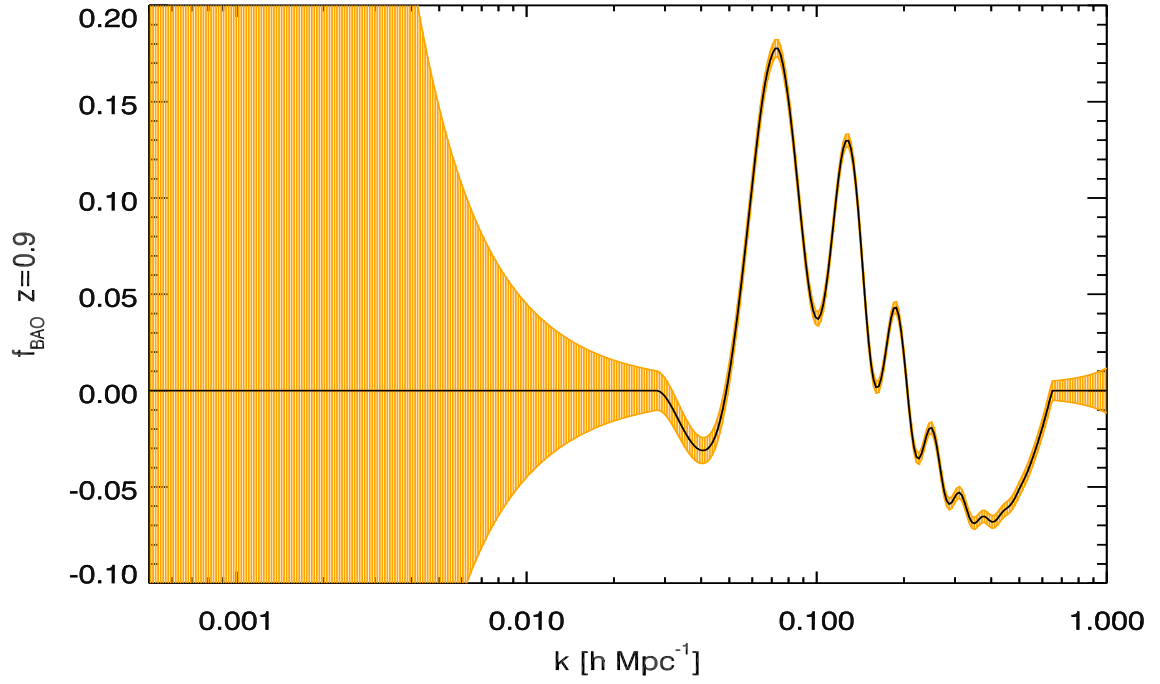


Figure 14. Example of the kind of BAO perturbations features with $f_{BAO} \pm \sigma_P/P$ errors that one could expect to obtain from FAST 21-cm intensity mapping. f_{BAO} is the ratio of the processed with BAO power spectrum to a power-law spectrum plus simple power law cut off for the processing suppression. f_{BAO} is forced to 0 outside the k range of interest so as not to consider the likely possible low k perturbations and the more non-linear effects at large k . σ_P/P are the anticipated fractional statistical errors on the matter power spectrum in the idealised survey. See figure 8 and 9 for examples.